Ceramics-Silikáty 70 (1), 34-41 (2026)
www.ceramics-silikaty.cz doi: 10.13168/cs.2025.0049

EFFECT OF MACHINED GRAPHITE MOULD COATINGS ON THE METALLURGICAL QUALITY OF TITANIUM ALLOY CASTINGS

#XIAO QIANGWEI*, **, WANG DEJI* , SUN CHU*, FU JINGYU*, FAN SHIXI*, #SHAHID HUSSAIN***, ****

*Beijing Institute of Aeronautical Materials Co., Ltd, Beijing 100094, China
**Beijing Engineering Research Center of Advanced Titanium Alloy Precision Forming Technology, Beijing 100094, China
***School of Materials Science and Engineering, Jiangsu University, Zhenjiang, 212013, China
****Department of Physics, University of Sargodha, Sargodha, 40100, Pakistan

#E-mail: shahid@ujs.edu.cn, x_qiangwei@163.com

Submitted September 23, 2025, accepted October 25, 2028

Keywords: Graphite mould, Surface-coating, Titanium alloy castings, Metallurgical quality

The poor surface metallurgical quality of machined graphite mould titanium alloy castings is one of the key issues limiting their application. A surface coating treatment was applied to the graphite mould, and its improvement effect was studied. Using small-batch titanium alloy nozzle shell castings as the subject, GSK fine-particle graphite was machined to prepare the mould, and an inert surface coating formulated from high-purity fused Y_2O_3 powder and zirconium acetate binder was applied. Comparative analysis experiments were conducted after casting. The focus was on exploring the coating's effects on the surface appearance, fluorescent defects, X-ray defects, and surface α layer of the titanium alloy castings. After surface coating the graphite mould, the surface roughness of the titanium castings decreased from 3.473~14.560 µm to 2.116~6.153 µm; the number of fluorescent defects decreased by 73.2 %, with linear defects reduced by 91.8 %; there was no significant difference in the internal defects of the castings; and the thickness of the surface α layer decreased from 185 µm to 136 µm. The surface coating can effectively improve the poor metallurgical quality of machined graphite mould titanium alloy castings and has good potential for promotion in engineering applications.

INTRODUCTION

Titanium and its alloys are characterised by their low density, high specific strength, heat and corrosion resistance, excellent stability, and non-magnetic properties, making them widely applicable in aerospace, marine, and chemical industries, among other fields. Near-net-shape and net-shape casting technologies enable the precision forming of complex structural components, offering advantages such as high material utilisation and low cost, and have become one of the important forming methods for titanium and its alloys [1–6]. Machined graphite mould casting technology, due to its high thermal stability, strong resistance to deformation, and short production cycle, is one of the most commonly used methods for titanium alloy casting [7–12]. However, because machined graphite moulds have high thermal conductivity, low density, and poor collapsibility, titanium alloy castings are prone to surface defects such as microcracks, cold shuts, and titanium nodules, which limit the further expansion of their application scope. To improve the surface quality of castings, applying coatings to the mould surface is an effective measure [13–16]. Y_2O_3 exhibits excellent inertness to high-temperature titanium alloy melts and is often used as a face coat material for investment precision casting of titanium alloys [17–24].

To further enhance the surface quality of titanium alloy castings produced by machined graphite moulds, Ning Erbin et al. [25] developed a face coat formulation with a ratio of Y_2O_3:binder:deionised water = 85:10:5, effectively improving the surface quality, dimensional accuracy, and metallurgical properties of titanium castings. Zhao Jun et al. [26–27] systematically studied the effects of refractory oxide coatings, such as ZrO_2, Y_2O_3, Al_2O_3, and $CaZrO_3$, on the surface quality, interfacial reactions, and surface microstructure and properties of titanium alloy specimens. Chang Huaqiang et al. [28] investigated the influence of Y_2O_3-silica sol system coatings on the mould-filling capability and casting quality of graphite mould casting. Yao Qian et al. [29] studied the effects of different Y_2O_3 coating methods on the interfacial layer microstructure and properties of titanium alloy castings.

The aforementioned studies demonstrate that surface coatings on machined graphite moulds can improve the quality of titanium alloy castings. However, there remains a lack of systematic comparative research on the effects of inert coatings on the metallurgical quality of titanium alloy castings in engineering applications. To address this gap, this study employs a coating system comprising high-purity fused Y_2O_3 powder and a zirconium acetate binder to prepare surface coatings for graphite moulds. [30-33] Using small-batch-produced titanium alloy nozzle casing castings as the research subject, we systematically investigate the influence of graphite mould surface coatings on the following aspects of ti-tanium castings: surface appearance, fluorescent inspec-tion defects, X-ray detectable defects and surface α-case layer formation.

Experimental

Material preparation

Casting and graphite mould design

The titanium alloy nozzle casing casting has dimensions of Ø 212 mm × 120 mm, a minimum wall thickness of 10 mm, and a weight of 3.6 kg, with a material grade of ZTC4. Figure 1 illustrates the casting structure and graphite mould design. The mould was fabricated using GSK fine-grained graphite, with key material parameters listed in Table 1.

Preparation of the inert coating

The surface inert coating was prepared using a high-purity fused Y_2O_3 powder and a zirconium acetate binder system. The specifications of the Y_2O_3 powder were as follows: Purity: ≥98 %, Particle size distribution: D_{90}: 300~400 mesh, D_{50}: 1,000~2,000 mesh. Coating preparation procedure: The fused Y_2O_3 powder and zirconium acetate solution were mixed at a mass ratio of 2:1. The mixture was stirred uniformly at room temperature for more than 30 minutes before use.

Graphite mould coating and aging process

The 20 sets of graphite moulds for the nozzle casings were randomly divided into two groups. One group of graphite moulds received a brush-applied surface coating treatment using the aforementioned face-coat slurry. During the coating process, special care was taken to ensure the complete coverage of all the mould surface areas that would contact the molten titanium alloy. Figure 2 illustrates the graphite moulds in both coated and uncoated states. After the coating dried, both groups of moulds were subjected to a firing treatment in a vacuum furnace, with the specific process parameters detailed in Table 2.

Casting melting and pouring

Both sets of graphite moulds were statically poured in a 100 kg vacuum consumable electrode skull furnace. The process utilised ZTC4 alloy ingots that had qualified through secondary melting. The specific melting process parameters are detailed in Table 3.

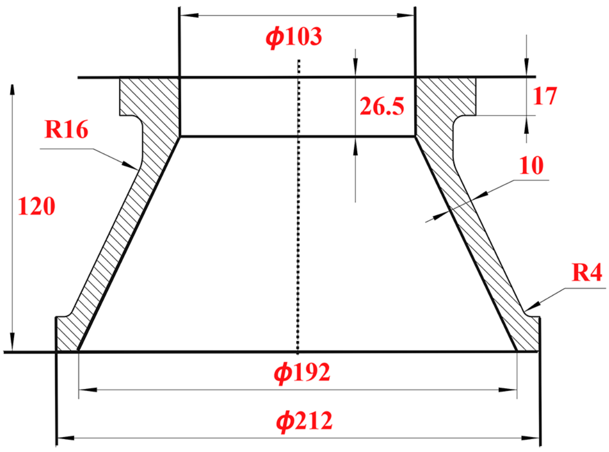

a)

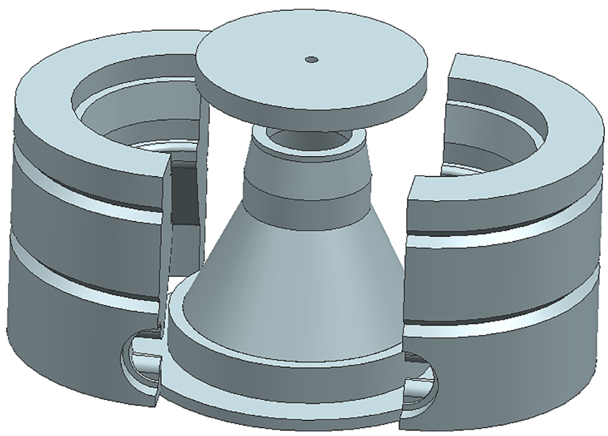
b)

Figure 1. Design drawings of the nozzle casing casting and its graphite mould: a) structural diagram of the nozzle casing casting, b) design drawing of the graphite mould for the nozzle casing.

Table 1. Performance of GSK graphite materials.

Particle (mm)	Density (g/cm^3)	Compressive strength (MPa)	Flexural strength (MPa)	Resistivity (μΩ·m)	Ash content (%)
0.8	1.75	25.4	16.8	9.5	≤0.3

Table 2. Sintering parameters of the graphite mould.

Vacuum level (Pa)	Temperature (°C)	Holding time (h)	Unloading temperature (°C)
≤6	900 ±20	2.5 ±0.5	≤ 300

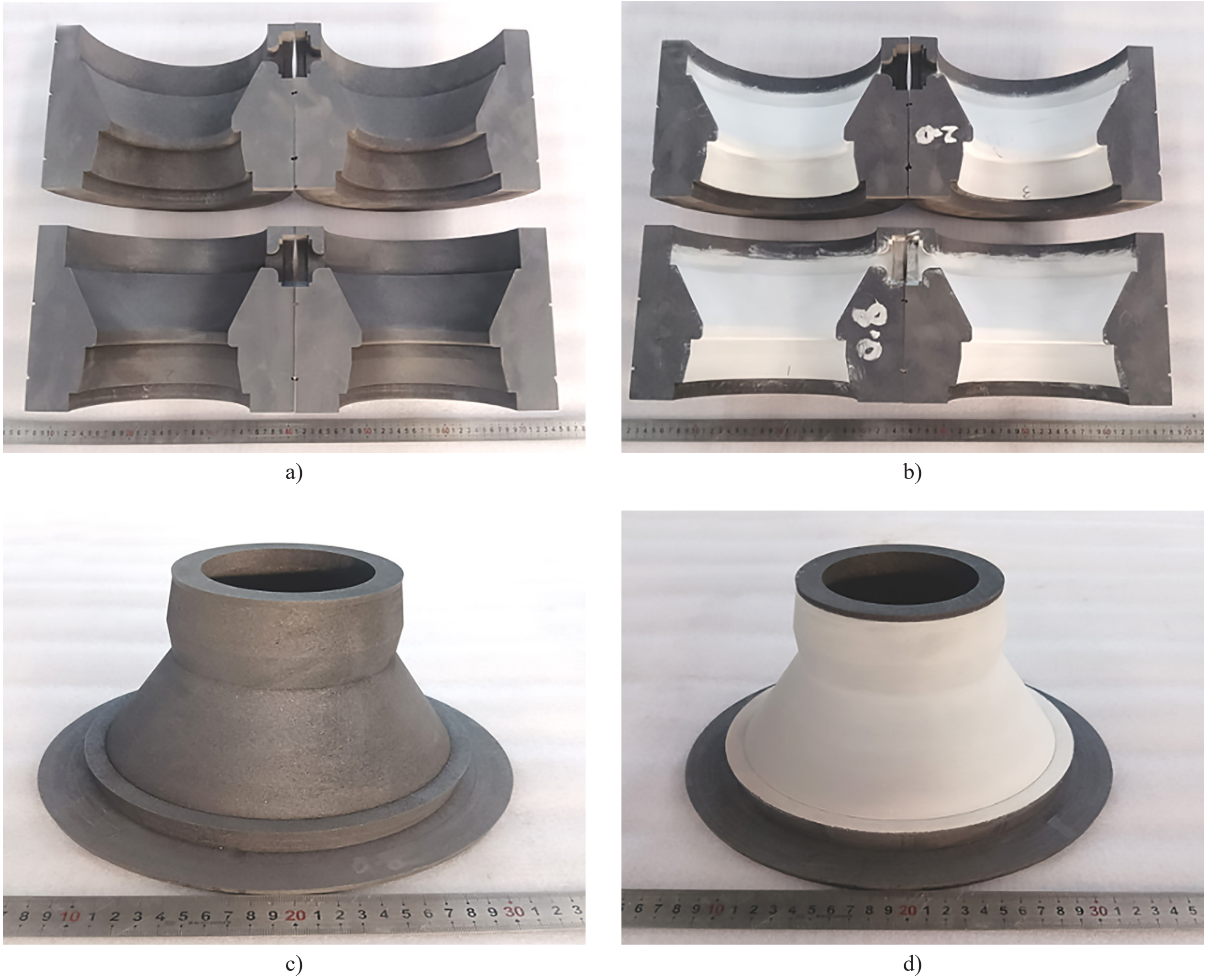

Figure 2. Schematic comparison of the graphite moulds before and after coating: a) uncoated graphite mould outer surface, b) coated graphite mould outer surface, c) uncoated graphite mould, d) coated graphite mould.

Table 3. The smelting process parameters.

Arc starting vacuum (Pa)	Melting vacuum (Pa)	Melting current (KA)	Melting voltage (V)	Cooling time (min)	Mould temp. (°C)
≤3.0	≤6.0	18~22	35~45	≥60	200

Analysis and testing methods

The surface conditions of the graphite moulds before and after coating were examined using a M205A stereo microscope. Surface roughness measurements were performed on typical areas of the castings using a Dailyaid DLSURF DR160 portable roughness tester, with 10 valid data points collected for each measurement. The thermal conductivity of both the graphite and Y_2O_3 materials was determined via the laser flash method using a LFA 427 Laser Flash Apparatus. For the surface quality inspection: fluorescent penetrant testing was conducted on a non-standard inspection line using: Penetrant: HM-604, Cleaner: Daraclean 282, Developer: D-90G powder. The internal quality of the castings was inspected using a Phoenix X cube XXL compact real-time X-ray imaging system for the non-destructive testing. Test specimens were extracted from a 10 mm-thick conical wall section of the casting, samples were mounted and prepared using: Primary etchant: 2 % HF + 4 % HNO_3 + 94 % H_2O (by volume), secondary etchant: 2 % NH_4HF_2 aqueous solution. The microstructural examination was conducted using a DM8000M metallurgical microscope.

RESULTS AND ANALYSIS

Surface appearance of castings

Figure 3 compares the surface quality of the castings produced by the coated and uncoated graphite moulds.

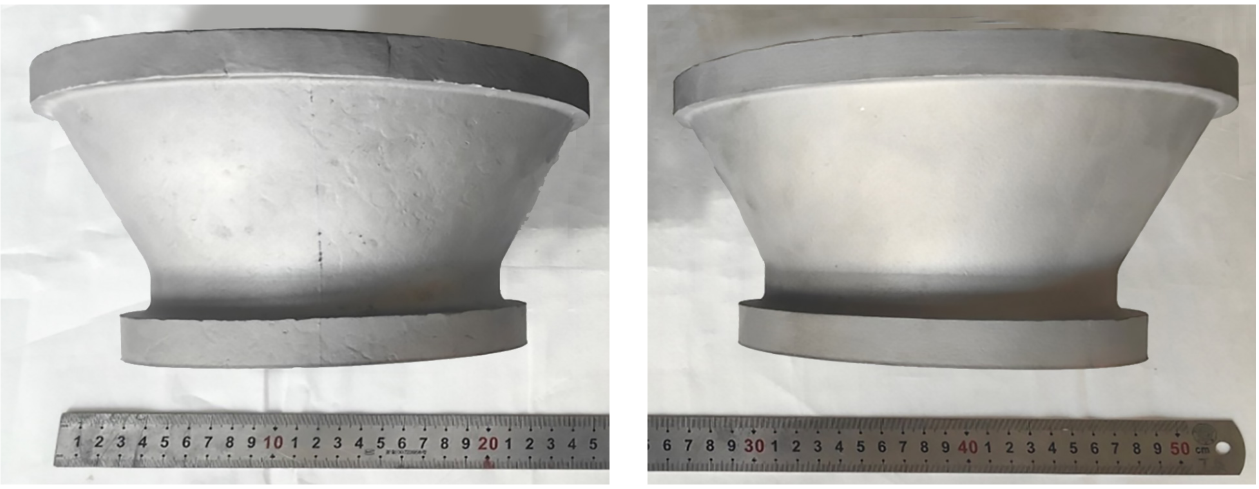

a) b)

Figure 3. Surface quality comparison of the castings: a) uncoated, b) coated.

The castings from the uncoated moulds exhibited significant surface defects including burrs, titanium nodules, flow marks, and even visually detectable cracks (Figure 3a). In contrast, the castings from the coated moulds showed markedly improved the surface quality with no visible defects (Figure 3b). Surface roughness measurements were conducted on one randomly selected casting from each group. Ten valid measurements were taken from representative surface areas of each casting (Table 4). The results demonstrate that: the surface roughness range improved from 3.473 ~ 14.560 μm to 2.116 ~ 6.153 μm; the average roughness decreased from 8.253 μm to 3.611 μm.

The visual inspection and surface roughness measurements clearly demonstrate that the coating treatment on the graphite moulds significantly improves the casting surface quality, substantially reducing the surface roughness and narrowing its variation range. This improvement is primarily attributed to the modified surface characteristics of the graphite moulds. As shown in Figure 4a, the GSK graphite material exhibits a microporous structure with notable regional variations in surface roughness. The excellent wettability between molten titanium and graphite enables the metal to penetrate into these pores during pouring, leading to surface defects such as burrs and titanium nodules. After the coating

Table 4. Surface roughness of the castings.

Condition	Surface roughness (μm)									
Uncoated	4.352	5.324	3.473	8.516	9.267	8.610	6.725	14.560	11.255	12.450
Coated	2.249	2.304	2.116	3.456	3.802	2.857	3.013	6.153	4.353	5.802

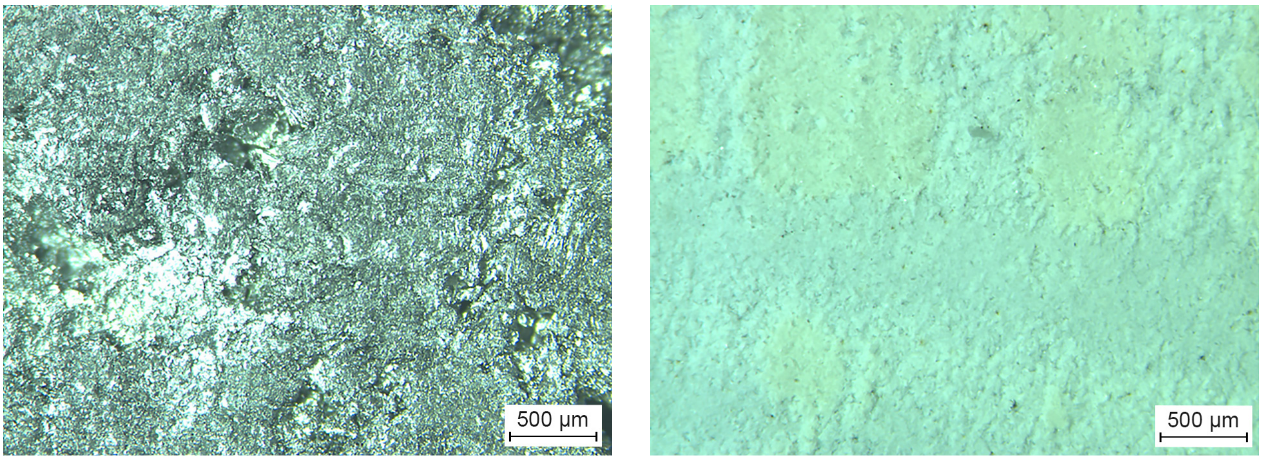

a) b)

Figure 4. Micrographs of graphite mould surfaces before and after coating: a) surface of the uncoated graphite mould, b) surface of the coated graphite mould.

application (Figure 4b), the surface micro-pores are effectively sealed, resulting in: 1) improved surface uniformity; 2) significant reduction in defect formation; 3) enhanced interfacial characteristics between the mould and molten metal.

Moreover, due to the graphite mould's high thermal effusivity and rapid heat conduction characteristics, the molten titanium experiences rapid chilling upon contact with the mould surface during filling, leading to defects such as flow marks and micro-cracks. The Y_2O_3 surface coating not only exhibits excellent high-temperature inertness, but also demonstrates significantly lower thermal conductivity than graphite. Figure 5 shows the temperature-dependent thermal conductivity curves of graphite and Y_2O_3. The thermal conductivity of graphite decreases significantly with the increasing temperature, while that of Y_2O_3 shows a slight increase, but remains at a relatively low level.

At 1150 °C, the thermal conductivity of graphite is about 60 times higher than that of Y_2O_3. This substantial

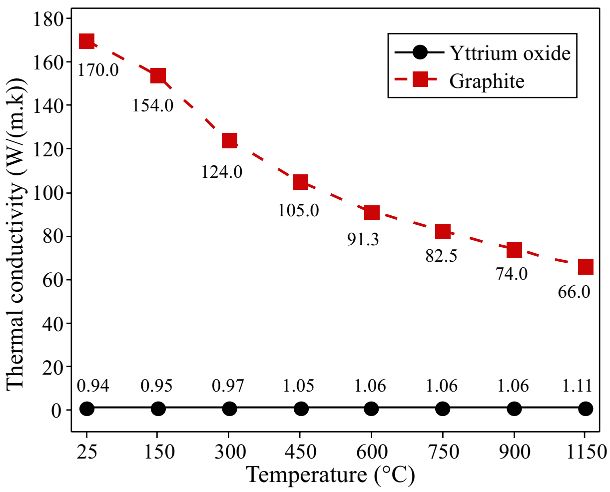

Figure 5. Thermal conductivity curves of graphite and yttrium oxide as a function of temperature.

thermal disparity enables the Y_2O_3 coating to function as an effective thermal barrier, creating a heat buffer zone between the molten titanium and the graphite mould. The coating effectively mitigates the cooling rate of titanium upon initial contact with the mould, thereby suppressing the formation of surface defects like flow marks and micro-cracks caused by rapid chilling.

The quality assessment of the titanium alloy nozzle casing castings was conducted using fluorescent penetrant inspection. The defect characteristics of castings produced with graphite-coated and uncoated moulds were statistically analysed and compared. Figure 6 shows a comparison of the fluorescent penetrant indications between typical castings from the two groups. It can be observed that the castings produced with uncoated moulds exhibited numerous linear defects and point-like defects, while the defect count significantly decreased in the castings treated with the coating. Figure 7 presents a comparative chart of the linear defects and total defect counts between the two groups of castings. For the 10 nozzle casings produced with the uncoated moulds, the total fluorescent defect count ranged from 24 to 67, with the linear defects numbering between 12 and 27. In contrast, the coated castings showed significantly fewer defects, with the total fluorescent defects ranging from 5 to 17 and linear defects numbering only 0 to 6.

The fluorescent penetrant testing results demonstrate that the nozzle casings produced with the coated moulds exhibited a remarkable reduction in the average defect count from 37.0 to 9.9, representing a 73.2 % decrease. Specifically, the average number of linear defects dramatically dropped from 20.7 to 1.7 (a 91.8 % reduction), while point-like defects decreased from 16.3 to 8.2 (a 49.7 % reduction).

Internal inclusions in the castings

Before hot isostatic pressing (HIP), real-time imaging was used to detect defects in the two groups of

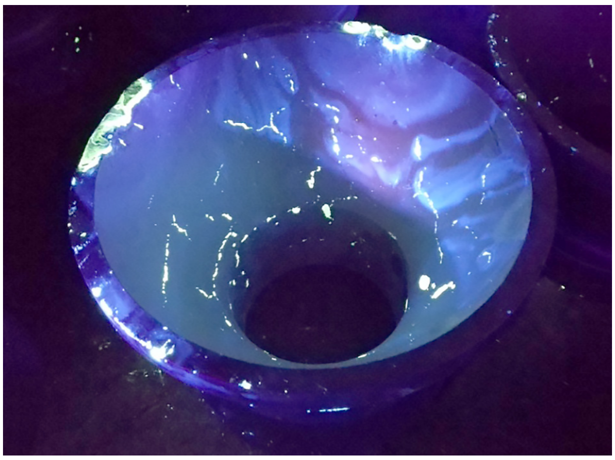

a)

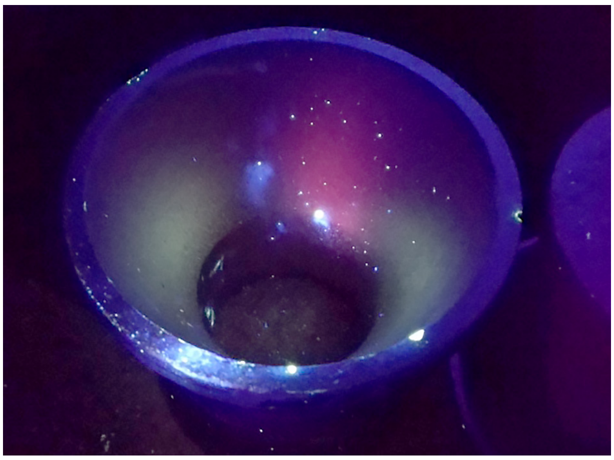

b)

Figure 6. Fluorescence quality of the casting surface before and after the mould brushing: a) uncoated, b) coated.

castings. Figure 8 shows the real-time radiographs of typical areas of the castings. As seen in Figure 9, both groups of castings exhibited scattered shrinkage porosity and micro-shrinkage. The uncoated castings showed localised crack indications (Figure 8a), with their locations partially overlapping with fluorescent linear defects. However, no inclusions were observed in either group.

After the HIP treatment, the internal shrinkage porosity and micro-shrinkage in both groups of castings were fully healed, and no defects were visible in the radiographs. These test results indicate that the graphite coating maintains excellent structural stability under the impact of high-temperature molten metal, with no coating detachment or other adverse phenomena observed in the coated castings. This outcome can be attributed to the coating's unique bonding mechanism: the graphite moulds commonly used in titanium alloy casting have a distinct microporous surface structure. During the coating process, the slurry fully infiltrates and fills these surface pores. After high-temperature sintering, the inert coating forms a strong mechanical interlocking structure with the graphite substrate. This "pinning effect" significantly enhances the coating's bonding strength, providing outstanding resistance to thermal shock at high temperatures. [34-37]

Surface α-layer in the castings

Figure 9 shows the characteristics of the α-layer in typical regions of titanium alloy nozzle casing castings prepared with coated and uncoated graphite moulds. As seen in Figure 9, both sample groups exhibited a distinct α-layer, but the mould coating influenced its thickness.

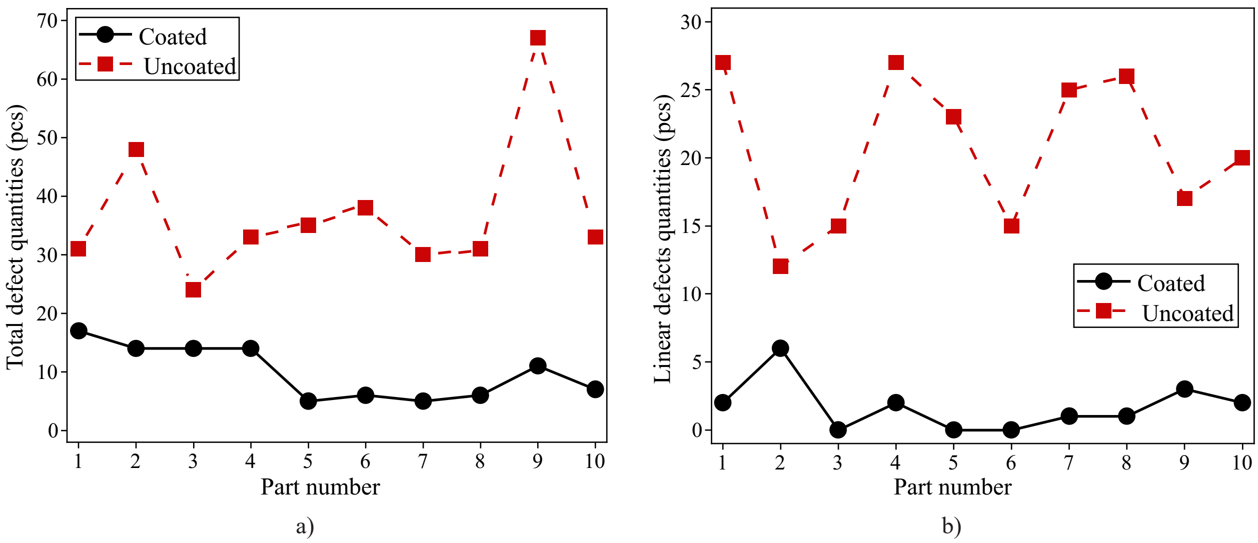

Figure 7. Comparison of the number of defects in the graphite versus unbrushed castings: a) comparison of the linear defect quantities in the castings, b) comparison of the total defect quantities in the castings.

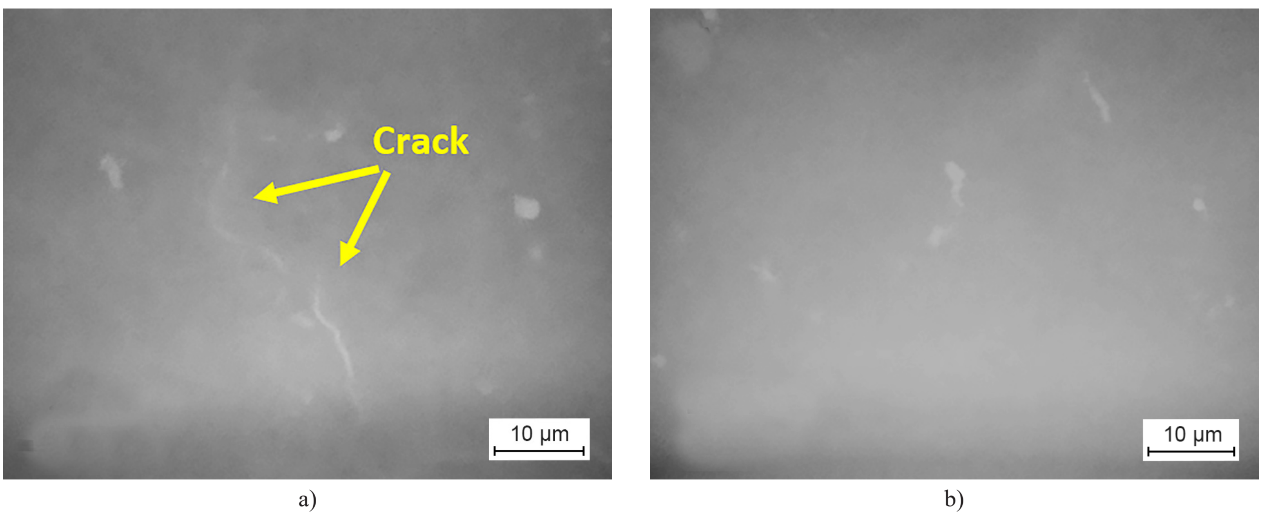

Figure 8. Radiographs of the internal defects in the castings before and after the mould coating: a) uncoated and b) coated.

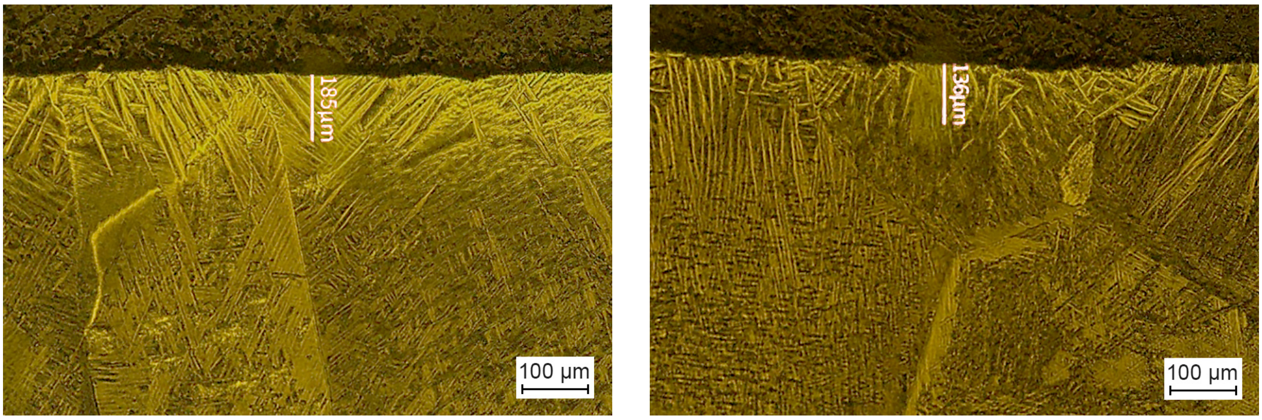

a) b)

Figure 9. Comparison of the α case of graphite brushed and unbrushed castings: a) uncoated and b) coated.

The uncoated sample has a α-layer thickness of 185 µm, while the coated sample measures 136 µm, representing a 26.5 % reduction in the thickness. This reduction can be attributed to the diffusion-inhibiting effect of the Y_2O_3 coating. From a thermodynamic perspective, although graphite materials possess excellent thermochemical stability and high refractoriness resulting in minimal interfacial reactions with molten titanium alloys, which helps control the α-layer thickness, they still struggle to completely block the diffusion of α-stabilising elements such as O and C. The inert coating employed in this study primarily consists of high-purity fused Y_2O_3, which demonstrates outstanding thermal stability. By forming a diffusion barrier between the molten titanium and graphite substrate, it reduces the elemental diffusion flux, thereby suppressing the formation and growth of the α-phase to some extent and ultimately decreasing the α-layer thickness. [38-41]

CONCLUSIONS

The castings produced using coated graphite moulds exhibited significantly fewer visual defects, with the surface roughness reduced from 3.473~14.560 µm to 2.116~6.153 µm. The total number of fluorescent defects decreased by 73.2 %, with the linear defects reduced by 91.8 %. The X-ray inspection confirmed that both the coated and uncoated groups of castings met the acceptance criteria in a single check after hot isostatic pressing, with no inclusions or other abnormal defects detected. The coating on the graphite surface demonstrated excellent impact resistance and thermal stability. The surface α-layer thickness of castings from the coated graphite moulds was 136 µm, compared to 185 µm for the uncoated castings. This confirms that the graphite surface coating effectively reduces the α-layer thickness in castings.

REFERENCES

1. Leyens C., Peters M. (2003). *Titanium and titanium alloys.* Wiley VCH, Weinheim, pp. 263–272. doi: 10.1002/ 3527602119.ch1
2. Senopati G., Rahman Rashid R. A., Kartika I., Palanisamy S. (2023): Recent development of low-cost β-Ti alloys for biomedical applications: a review. *Metals*, *13*(2), 194. doi: 10.3390/ met13020194
3. Kaliuzhnyi P., Voron M., Mykhanian O., Tymoshenko A., Neima O., Iangol O. (2021): Interaction of titanium with ceramic molds in the conditions of electron beam casting technology. *Archives of Foundry Engineering*, *21*(3), 27-32. doi: 10.24425/ afe.2021.136109
4. Jörg F., Betül K. A., Heiner M., Gerhard K., Erwin B. R. (2020): Effects of ti6al4v surfaces manufactured through precision centrifugal casting and modified by calcium and phosphorus ion implantation on human osteoblasts. *Metals*, *10*(12), 1681. doi: 10.3390/met10121681
5. Marin E., Lanzutti A. (2023): Biomedical applications of titanium alloys: a comprehensive review. *Materials*, *17*(1), 114. doi: 10.3390/ma17010114
6. Yu W., Li J., Li H., Shi F., Wu G. (2024): Investigation into relationships between grain size distribution characteristics and mechanical properties in large-scaled complex titanium alloy castings utilizing LASSO regression. *Journal of Alloys and Compounds*, *977*, 173409. doi: 10.1016/j.jallcom.2023. 173409
7. Sadayappan M., Sahoo M., Lavender C., Jablonski P. (2008): Permanent mold casting of titanium alloy Ti–6Al–4V. *International Journal of Metalcasting*, *2*(1), 69-74. doi: 10.1007/ BF03355423
8. Cheng W. W., JU C. P., Lin J. C. (2007): Structure, casta-bility and mechanical properties of commercially pure and alloyed titanium cast in graphite mould. *Journal of Oral Rehabilitation*, *34*(7), 528-540. doi: 10.1111/j.1365-2842.2003.01151.x
9. Wang L., Yan H., Teng J., Liu X., Wang X., Su Y., Guo J. (2020): Effect of hydrogen on interfacial reaction between Ti–6Al–4V alloy melt and graphite mold. *Journal of Ma-terials Research and Technology*, *9*(3), 6933-6939. doi: 10.1016/j.jmrt.2020.02.071
10. Jia L., Xu D., Li M., Guo J., Fu H. (2012): Casting defects of Ti–6Al–4V alloy in vertical centrifugal casting processes with graphite molds. *Metals and Materials International*, *18*(1), 55-61. doi: 10.1007/s12540-012-0007-0
11. Valenza F., Gambaro S., Bigos A., Czaja P., Janusz-Skuza M., Wojewoda-Budka J. (2023): Wetting and interfacial reactivity of graphite by liquid TiCuNi. *Surfaces and Interfaces*, *41*, 103323. doi: 10.1016/j.surfin.2023.103323
12. Yang Y., Wang X., Li X., Zhou R., He Z., Jiang Y. (2023): Numerical simulation on solidification during vertical centrifugal

casting process for TC4 alloy wheel hub with enhanced mechanical properties. *Materials*, *17*(1), 184. doi: 10.3390/ma17010184

13. Tuttle R., Ramrattan S., Wells L., Medved J. (2022): Refractory coated surface characterization for steel using disk-shaped chemically bonded sand specimens – Part II. *International Journal of Metalcasting*, *16*(2), 493-501. doi: 10.1007/s40962-021-00618-3
14. Zheng K. K., Lin Y. X., Yan S. Q., Chen W. P. (2023): Research on surface coating treatment of casting die for copper alloy water-meter shell. *International Journal of Metalcasting*, *17*(2), 922-934. doi: 10.1007/s40962-022-00819-4
15. Lopes V., Puga H., Barbosa J., Teixeira J. C. (2020): Effect of yttria mould coating on the investment casting of AZ91D-1 wt% CaO magnesium alloy. *International Jour-nal of Metalcasting*, *14*(1), 98-107. doi: 10.1007/s40962-019-00339-8
16. Jafari H., Idris M. H., Ourdjini A., Karimian M., Payganeh G. (2010): Influence of gating system, sand grain size, and mould coating on microstructure and mechanical pro-perties of thin-wall ductile iron. *Journal of Iron and Steel Research, International*, *17*(12), 38-45. doi: 10.1016/S10 06-706X(10)60195-1
17. Chen A., Ma Y., Wang Z. F., Liu H., et al. (2024): Pre-paration of yttrium oxide coating with enhanced thermal shock resistance on refractories used for titanium alloy melting and casting. *Journal of Iron and Steel Research International*, *31*(6), 1411-1422. doi: 10.1007/s42243-023-01070-9
18. Jia Z., Xu X., Guo X., Fan H., et al. (2025): High-purity Y_2O_3 ceramic cores with enhanced chemical compatibility in investment casting of titanium alloys. *Journal of Alloys and Compounds*, *1021*, 179670. doi: 10.1016/j.jallcom.2025.179670
19. Li C., Li M., Zhang H., Ali W., Qin Z., Wang H., Lu X. (2017): Fabrication of Y_2O_3 doped $BaZrO_3$ coating on Al2O3 applied to solidification of titanium alloy. *Surface and Coatings Technology*, *320*, 146-152. doi: 10.1016/j.surfcoat.2017.01.079
20. Freitag L., Schafföner S., Faßauer C., Aneziris C. G. (2018): Functional coatings for titanium casting molds using the replica technique. *Journal of the European Ce-ramic Society*, *38*(13), 4560-4567. doi: 10.1016/j.jeurce-ramsoc.2018.05.020
21. Uwanyuze R. S., Kanyo J. E., Myrick S. F., Schafföner S. (2021): A review on alpha case formation and modeling of mass transfer during investment casting of titanium alloys. *Journal of Alloys and Compounds*, *865*, 158558. doi: 10.1016/j.jallcom.2020.158558
22. Neto R. L., Duarte T. P., Alves J. L., Barrigana T. G. (2017): The influence of face coat material on reactivity and fluidity of the Ti_6Al_4V and TiAl alloys during invest-ment casting. *Proceedings of the Institution of Mecha-nical Engineers, Part L: Journal of Materials: De-sign and Applications*, *231*(1-2), 38-48. doi: 10.1177/ 1464420716681824
23. Yang L., Feng Q., Tang S., Ling Q., Liu X., Fan Z. (2023): Effect of $CaTiO_3$ on sintering properties of Y_2O_3-based ceramic shell via extrusion-based 3D printing for titanium alloy casting. *Ceramics International*, *49*(11), 19338-19345. doi: 10.1016/j.ceramint.2023.03.061
24. Guo X., Fan H., Wang N., Li X., et al. (2025): Improved leachability of CaO modified Y_2O_3 ceramic cores for investment casting of titanium alloys. *Journal of Alloys and Compounds*, 181252. doi: 10.1016/j.jallcom.2025.181252
25. Ning E. (2007). An auxiliary process for improving qua-lity of graphite mold titanium alloy castings. China: CN2007103004042.7.
26. Zhao J., Zhang J., Lei J. (2017): Research on properties of ZrO_2 coating for titanium alloy graphite mold casting, *Foundry, 66*(6), 563–567.
27. Zhao J., Zhang J., Jin L., Liu SB., et al. (2017): Effects of coating material on machining, graphite casting process forming quality of Ti Alloy. *Rare Metal Materials and Engineering, 46*(1), 190–194.
28. Chang HQ., Ji ZL., Mu XH., Sun HZ., Li BB. (2022): Application of coating technology graphite casting of titanium alloy. *Special Casting & Nonferrous Alloys, 42*(05), 652–654.
29. Yao Q., Liu T., Liu S., Li C., Shi K. (2024):, Effect of coating on microstructure and properties of interfacial layer of graphite cast titanium alloy. *Materials Reports, 38*(Z2), 24080027.
30. Hua L., Du Y., Qian D., Sun M., Wang F. (2025): Influence of Prior Cold Rolling on Bainite Transformation of High Carbon Bearing Steel. Metallurgical and Materials Transactions A, 56(2), 640-654. doi: 10.1007/s11661-024-07669-1
31. Tang H., Peng J., Peng H., Yang Y., Gao Q., Xiao L., Yang Z. (2025): Test and Theoretical Investigations on Flexural Behavior of High-Performance H-Shaped Steel Beam with Local Corrosion in Pure Bending Zone. *Steel research international, 96*(7), 2400640. doi: 10.1002/srin.202400640
32. Liu Y., Zhu L., Ma G., Lu Y., Wei A., Yang C., Wang H. (2025): Tribocorrosion behaviours and mechanisms of Inconel 625–nano/micro Al_2O_3 composite coatings prepared by plasma enhanced high-velocity arc spraying. *Corrosion Science, 256*, 113221. doi: 10.1016/j.corsci.2025.113221
33. Huang Y., Xie Y., Chen J., Li J., Zhao Y., Meng X. (2025) : Wire-based friction stir additive remanufacturing of 2219 aluminum alloy components. *The International Journal of Advanced Manufacturing Technology, 137*(11), 6029-6041. doi: 10.1007/s00170-025-15544-5
34. Dong W., Meng X., Xie Y., Zhang Z., Tian H., Sun X., Huang Y. (2025): Wire-based friction stir welding enables equal-strength joining of aluminum alloys even with assembling gaps. *Journal of Manufacturing Processes, 151*, 426-433. doi: 10.1016/j.jmapro.2025.07.050
35. Zou Y., Tang S., Guo S., Song X. (2024). Tool wear analysis in turning inconel-657 using various tool materials. *Materials and Manufacturing Processes, 39*(10), 1363-1368. doi: 10.1080/10426914.2024.2323434
36. Shao L., Li W., Lu Q., Xue N., Chen Y., Wu Y., Zhu L. (2025): Bonding mechanism in Cu coating deposited on Al alloy substrate: Combining molecular dynamics simulation and experiment. *Materials Science and Engineering: A, 942*, 148703. doi: 10.1016/j.msea.2025.148703
37. Hu J., Li X., Meng Q., Wang L., Li Y., Xu W. (2022): Tailoring retained austenite and mechanical property improvement in Al-Si-V containing medium Mn steel via direct intercritical rolling. *Materials Science and Engineering: A, 855,* 143904. doi: 10.1016/j.msea.2022.143904
38. Shen C., Wang C., Wei X., Li Y., van der Zwaag S., Xu W. (2019): Physical metallurgy-guided machine learning and artificial intelligent design of ultrahigh-strength stainless steel. *Acta Materialia, 179*, 201-214. doi: 10.1016/j.actamat.2019.08.033
39. Zhao Y., Ma H., Sun J., Luo J., Su Y., Feng L., Liaw P.K. (2025): A Xanthium sibiricum biomimetic Fe-based medium-entropy alloy with significant antibacterial and mechanical behaviors. *Rare Metals, 44*(7), 4913-4935. doi: 10.1007/s12598-024-03097-7
40. Qin X., Wang Q., Zhao X., Xia S., Wang L., Zhang Y., Jiang B. (2025): PCS: Property-composition-structure chain in Mg-Nd alloys through integrating sigmoid fitting and conditional generative adversarial network modeling. *Scripta Materialia, 265*, 116762. doi: 10.1016/j.scriptamat.2025.116762
41. Shi S., Zhao Y., Lin X., Deng H., Zhao L., He G., Huang W. (2025): Significance of α-Al cellular matrix in tensile behavior and work-hardening of additive manufactured $AlSi_{10}Mg$ alloy. *Virtual and Physical Prototyping, 20*(1), e2449189. doi: 10.1080/17452759.2024.2449189